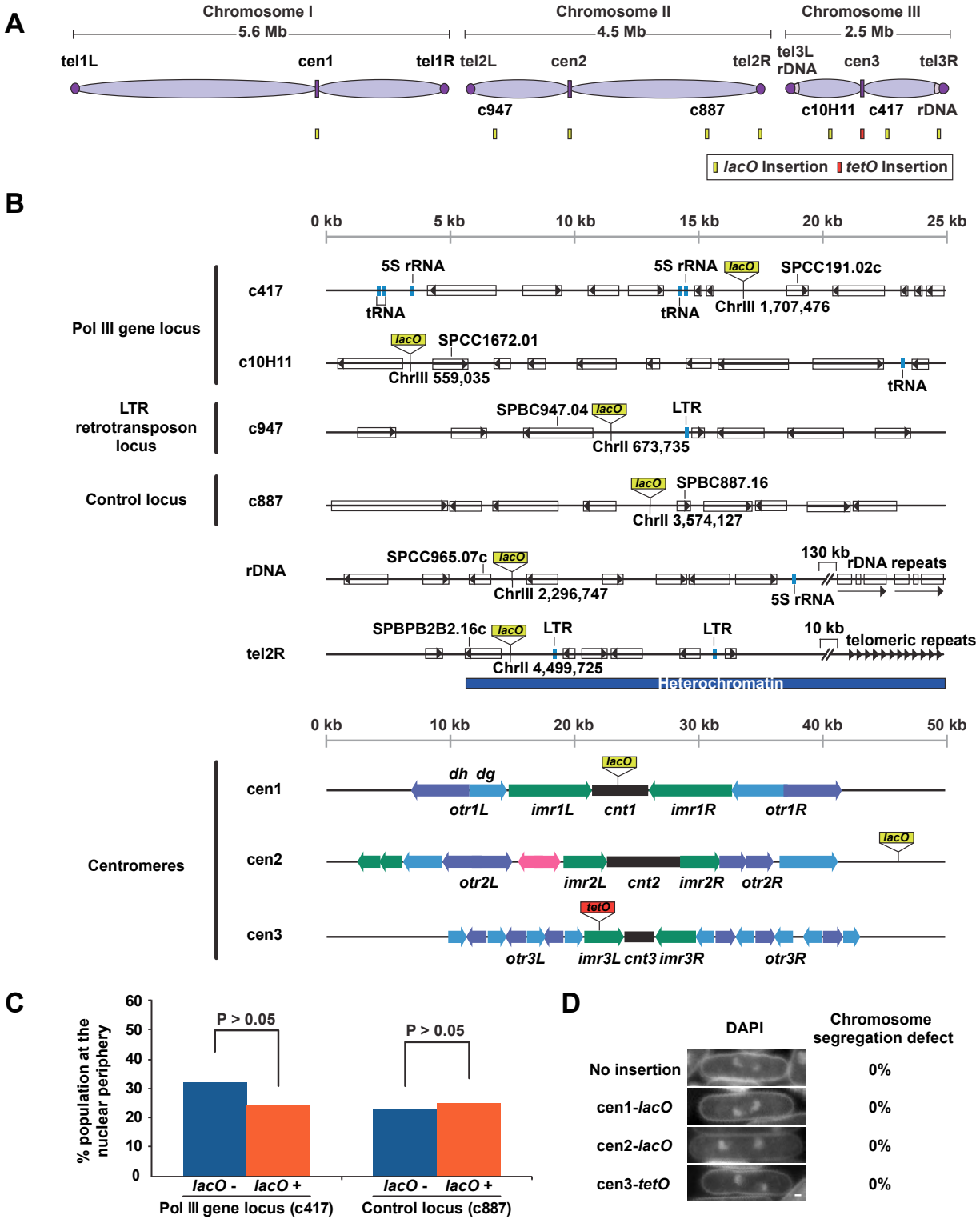

Fig. S1. The insertions of *lacO*/*tetO* repeats did not affect intra-nuclear positioning of the genomic loci in relation to the nuclear periphery. (A) The genome-wide locations of the *lacO*/*tetO*-repeats insertions. (B) The detailed annotation of the *lacO*/*tetO*-repeats insertions employed for live-cell imaging analyses. (C) FISH analysis was performed as described (Sadaie et al., 2003) to visualize the c417 Pol III gene locus and the c887 control locus in cells with or without *lacO* repeats at the respective loci. The c417 and c887 cosmid clones were used for preparing FISH probes specific to the Pol III gene locus and the control locus, respectively (Mizukami et al., 1993). Nucleoplasm was also visualized by DAPI staining. FISH foci overlapping with the edges of DAPI signal were counted as peripheral localization. FISH images were captured by a Zeiss Axioimager Z1 fluorescence microscope with an oil immersion objective lens (Plan Apochromat, 100X, NA 1.4, Zeiss). Images were acquired at 0.2 μm intervals in the *z*-axis and deconvolved by Axiovision 4.6.3 software (Zeiss). More than 100 cells were analyzed for each experiment. (D) Cells carrying the *lacO*/*tetO* insertions at the centromeres (cen1, cen2, and cen3) do not show chromosome segregation defects. The indicated strains were stained by DAPI and more than 500 cells were analyzed to determine whether the insertions cause chromosome segregation defects. The scale bar indicates 1 μm.

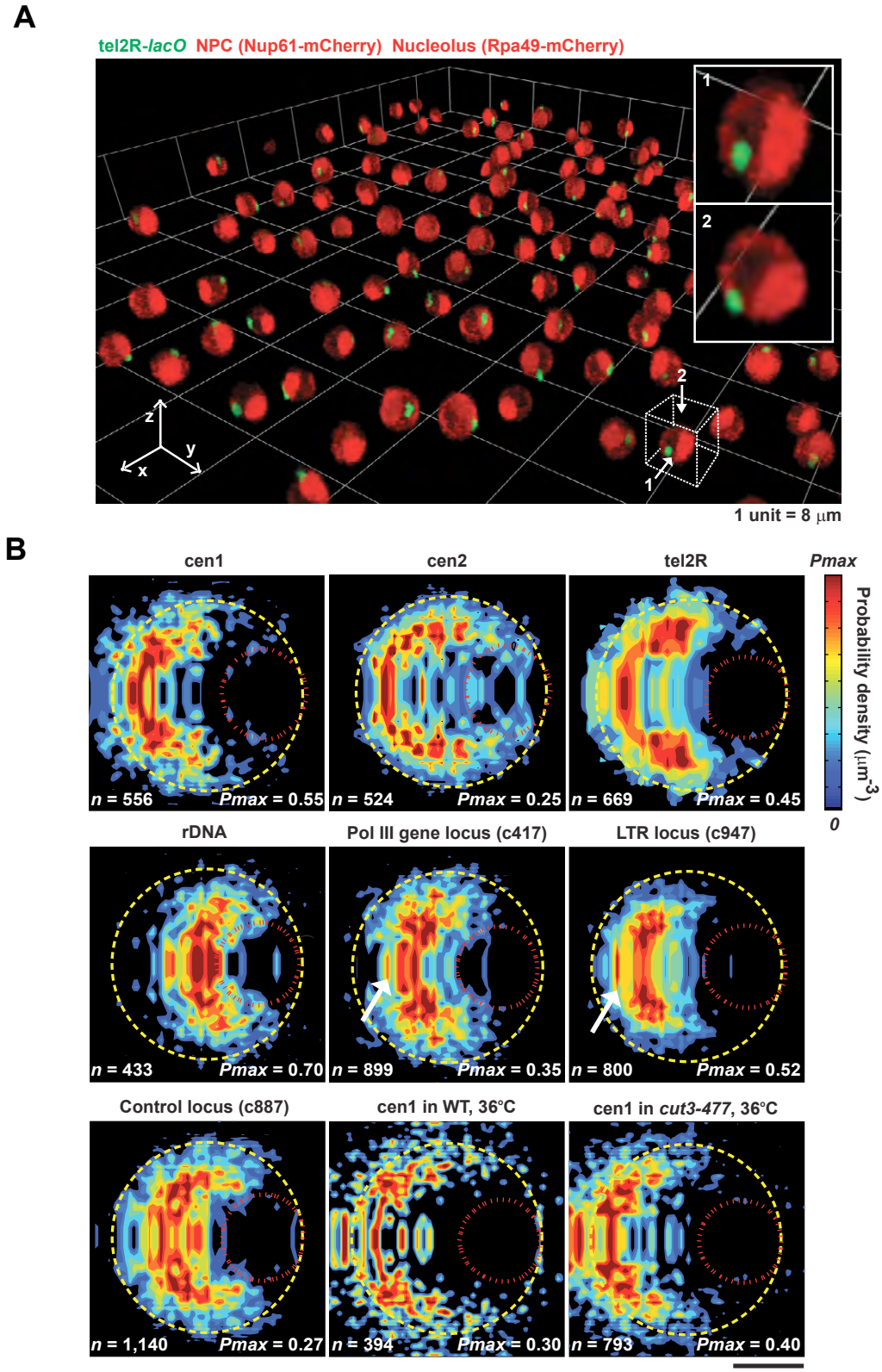

Fig. S2. Probability density maps of the fission yeast genomic loci. (A) Three-dimensional positioning of the tel2R telomere locus in the live fission yeast nuclei. The telomeric locus carrying *lacO* repeats (green) was visualized with the nuclear landmarks (red) such as the nuclear pore complex (NPC) and the nucleolus. The representative nucleus in the box was enlarged, rotated, and presented from two angles (1 and 2) to show typical positioning of the telomeric locus. (B) Probability density maps of the centromeres (cen1 and cen2), the telomere (tel2R), the rDNA locus, the Pol III gene locus (c417), the LTR retrotransposon locus (c947), and the control locus (c887). Probability density mapping of fluorescently labeled genomic loci was performed as previously described, with slight modifications (Berger et al., 2008). Mapping of cen1 was also performed in wild-type and *cut3-477* condensin mutant cells, which were cultured at the restrictive temperature (36°C) for 2 hr. Most cells used for this analysis were in interphase. Dashed yellow and red lines represent the nuclear membrane and the nucleolus, respectively. Arrows indicate the loci juxtaposed to the centromere-occupied domain in the limited cell population. The color bar indicates probability density from 0 to Pmax. The scale bar indicates 1 μm.

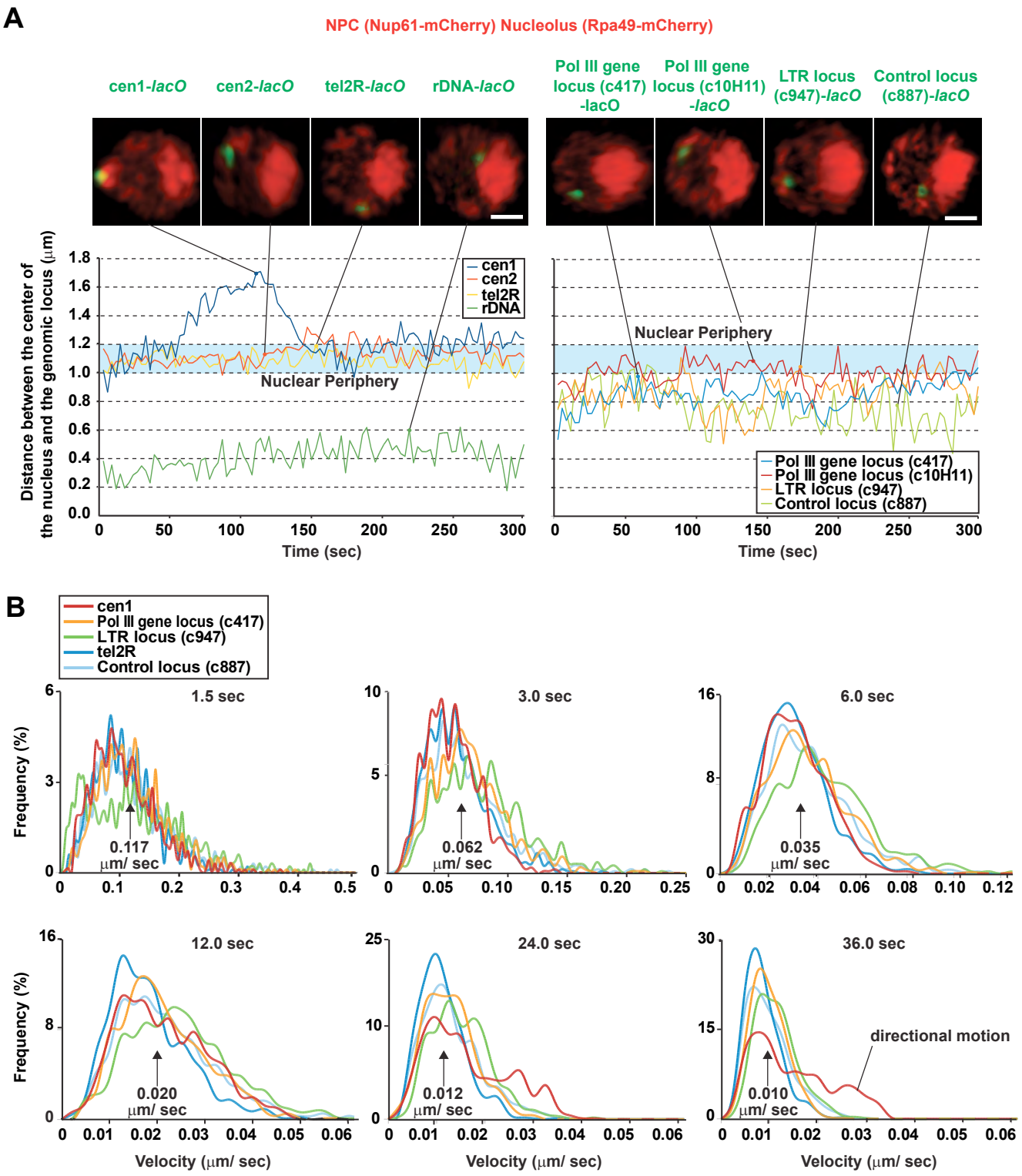

Fig. S3. Three-dimensional motion of several genomic loci in live fission yeast cells. (A) The genomic loci (green), such as the centromeres (cen1 and cen2), the telomere (tel2R), the rDNA locus, the Pol III gene loci (c417 and c10H11), the LTR retrotransposon locus (c947), and the control locus (c887), were visualized with the NPC (Nup61-mCherry, red) and the nucleolus (Rpa49-mCherry, red). Images were captured in 3D at 3.0-sec intervals for 5 min. The nuclear center was estimated in every image based on the NPC signals, and distances between the nuclear center and the respective genomic loci were plotted against time. Representative images at the indicated time points are shown on top. Scale bars indicate 1 μm. (B) Velocities of the centromere (cen1), the Pol III gene locus (c417), the LTR retrotransposon locus (c947), the telomere (tel2R), and the control locus (c887). The genomic loci were visualized with the NPC and the nucleolus in live cells. Three-dimensional images were captured in five cells at 1.5-sec intervals for 5 min. Intra-nuclear positioning of the respective genomic loci was determined in 3D time-lapse images. The center of the nucleus was used to remove potential effects derived from the migration of cells and nuclear shift in the cytoplasm. Moving distances of the respective genomic loci at the indicated intervals (top) were calculated and used to estimate velocities of the loci. Distributions of estimated velocities of the respective genomic loci were plotted. Average velocities considering all genomic loci are indicated under the arrows.

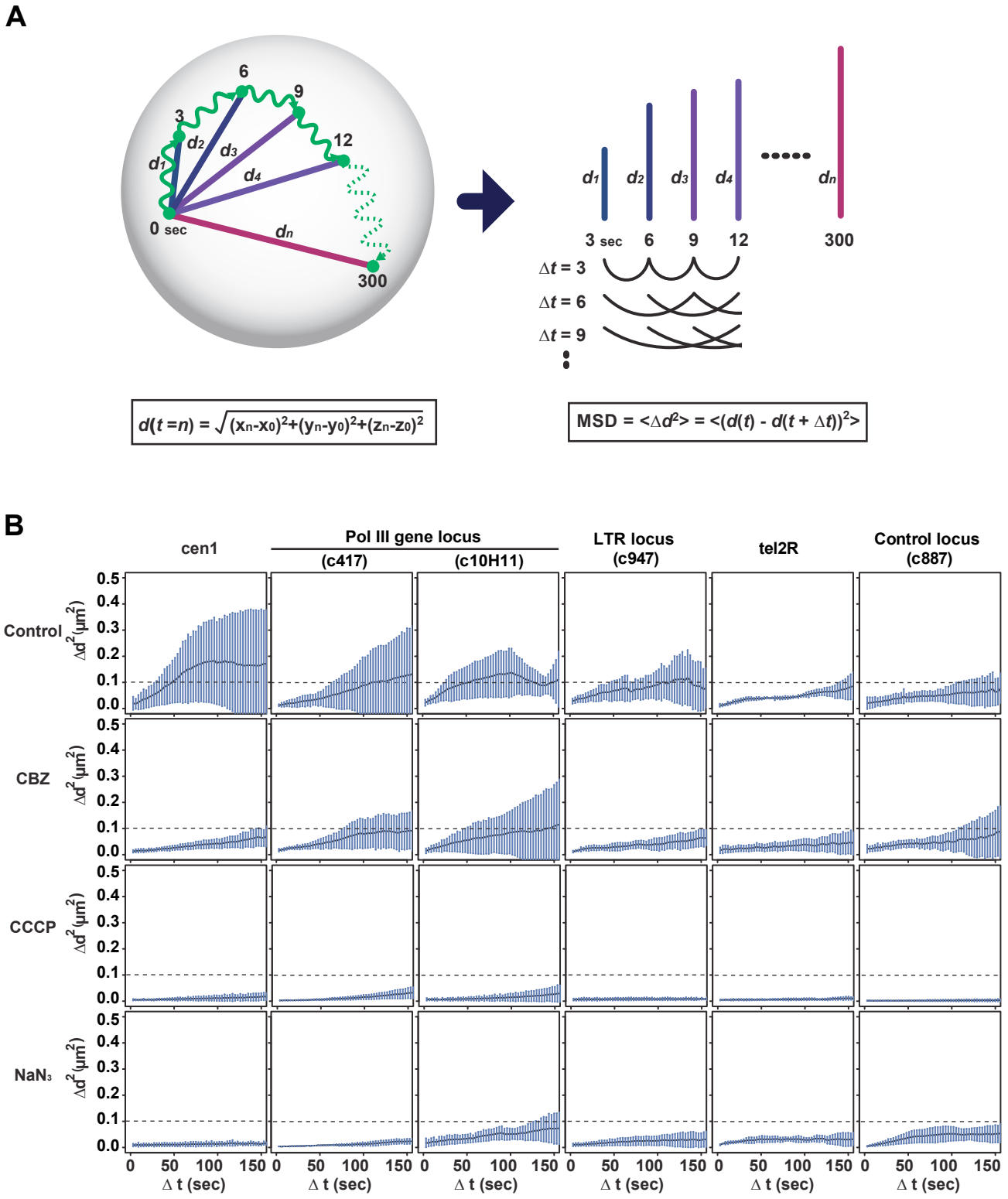

Fig. S4. Mean squared displacement analysis for the fission yeast genomic loci. (A) Estimation on mean squared displacement (MSD) of the genomic locus. MSD analysis was performed as previously described (Chubb et al., 2002; Heun et al., 2001; Marshall et al., 1997). Schematic briefly explains MSD analysis. The 3D displacement (Δd μm) of the genomic locus was estimated with incrementing intervals (Δt) from 0 to 150 sec. The squared displacement of the genomic locus was calculated as Δd2= (d(t)-d(t+Δt))2 in five cells. The mean values of the squared change of distance <Δd2> were calculated with incrementing intervals and plotted against Δt. (B) MSD analysis was performed for the centromere locus (cen1), the Pol III gene loci (c417 and c10H11), the LTR retrotransposon locus (c947), the tel2R telomere locus, and the control locus (c887) in several culturing conditions. Cells were treated with 50 μg/ml CBZ, 40 mM CCCP, or 15 mM NaN3 in liquid EMM for 15 min and applied to microscopic slides. The genomic loci (*lacO*, green), NPC (Nup61-mCherry, red), and the nucleolus (Rpa49-mCherry, red) were co-visualized in live cells. The position of the genomic loci was normalized by the center of the nucleus. The graphs represent averages from five cells (± s.d.).

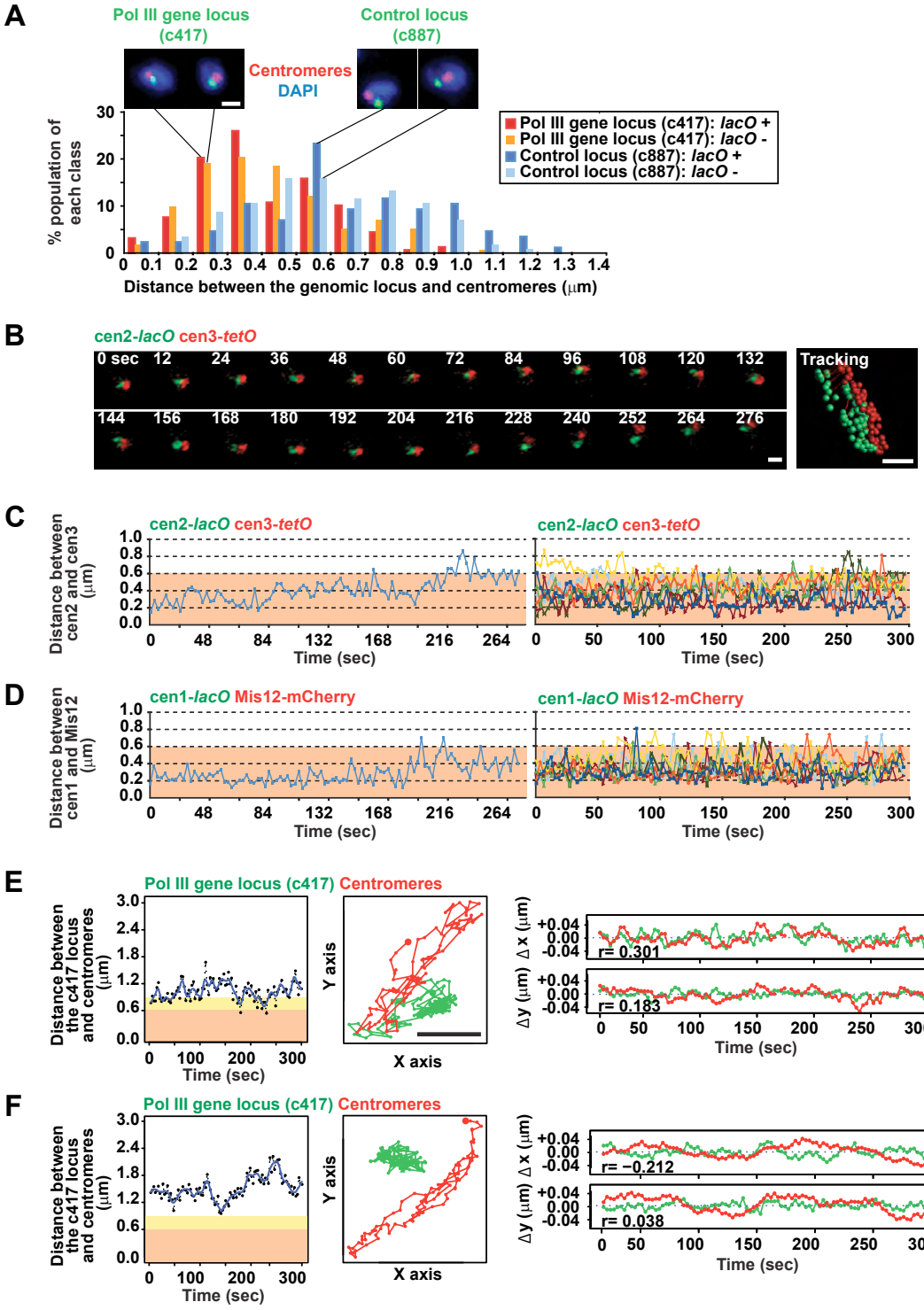

Fig. S5. Evaluation of potential associations between centromeres and the genomic loci. (A) FISH analysis was performed to visualize centromeres (red) and the genomic loci (green), such as the c417 Pol III gene locus and the c887 control locus, in cells with or without *lacO* repeats at the respective loci. Distances between centromeres and the genomic loci were measured and summarized in a graph. Typical images are shown on top. (B) Centromeres such as cen2 (green) and cen3 (red) were co-visualized in live cells. Images were captured in 3D at 3.0-sec intervals for 5 min and selected frames are shown. (C) Distances between cen2 and cen3 were measured in time-lapse images used in panel (B) (left). Distances between cen2 and cen3 were measured in seven cells and plotted against time (right). (D) Distances between cen1 and Mis12. Distances between cen1 and Mis12 were measured in seven cells and plotted against time (right). The representative result is also shown (left). (E) The c417 Pol III gene locus and centromeres show the coordinated movement where two foci transiently migrate within 0.9 μm during the 5-min investigation. Distances between the Pol III gene locus and centromeres were plotted against time (left). Tracking of the Pol III gene locus (green) and centromeres (red) along the x and y axes is shown (middle). Coordinates of the c417 Pol III gene locus and centromeres in x and y axes were used to calculate Δx and Δy at 3.0-sec intervals. The Δx and Δy values were plotted against time and used to calculate Pearson's correlations (right). (F) The c417 Pol III gene locus and centromeres do not show the coordinated movement in the cell carrying two foci continuously separated more than 0.9 μm during the 5-min investigation. Scale bars indicate 1 μm.

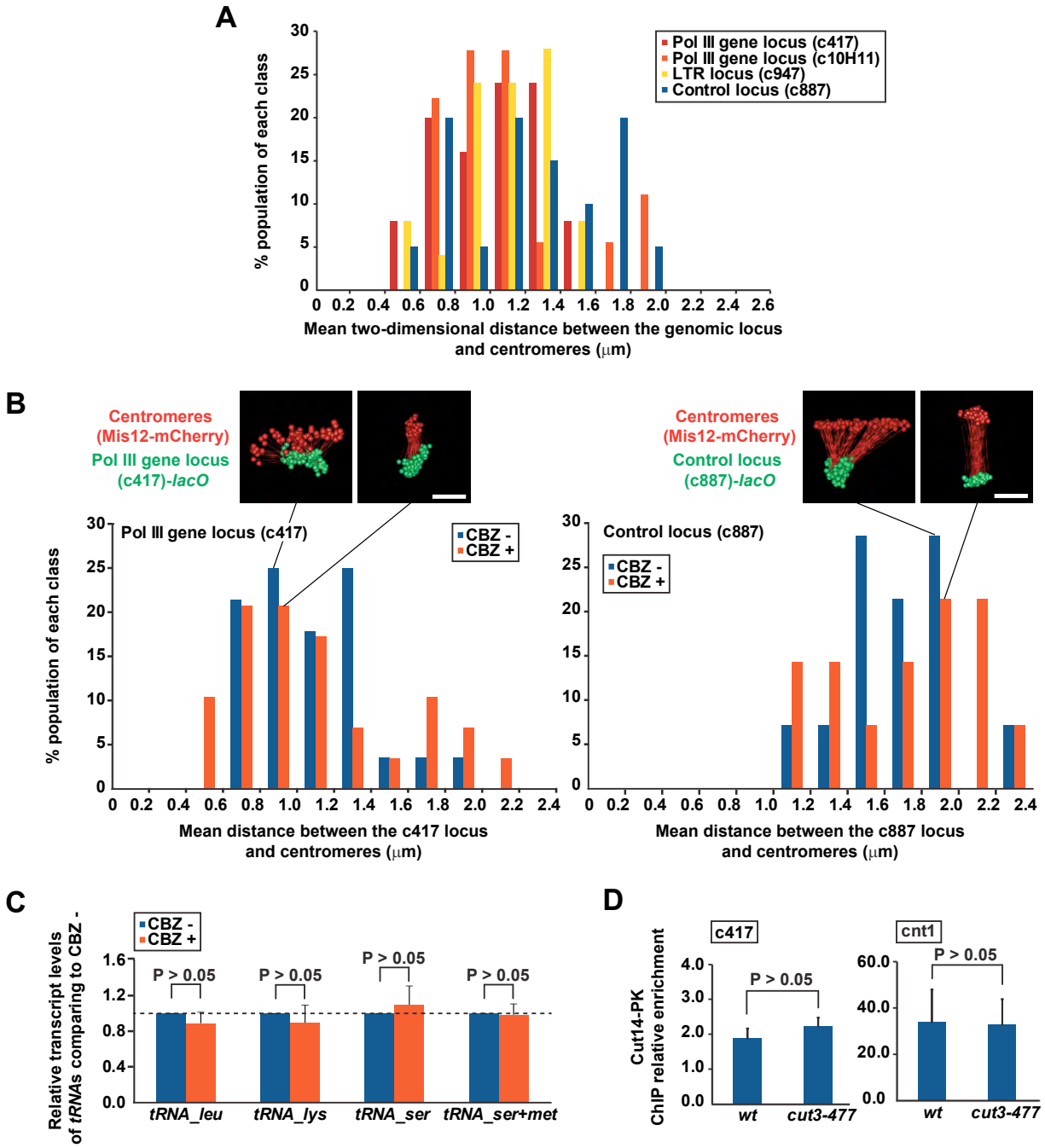

Fig. S6. CBZ treatment does not affect proximity of the Pol III gene locus to centromeres nor the transcriptional regulation of Pol III genes. (A) Distributions of mean distances between centromeres and the indicated genomic loci in cell populations. Images were captured at 3.0-sec intervals for 5 min. Distances between centromeres and the genomic loci were measured in z-projection images (2D). Distances were monitored in more than 20 live cells and mean distance was calculated for each cell. Distributions of mean distances were plotted in the histogram. (B) Distributions of mean distances between centromeres (Mis12-mCherry, red) and the genomic loci (green) in the cell population. Cells were treated with 50 μg/ml CBZ in liquid EMM for 15 min and applied to microscopic slides with a mounting medium containing CBZ. Images were captured in 3D at 3.0-sec intervals for 5 min. Distances between centromeres and the genomic loci, such as the c417 Pol III gene locus and the c887 control locus, were measured in more than 20 live cells. Distributions of mean distances are summarized in a graph. Representative tracking images are shown on top. (C) Transcript levels of Pol III genes were quantified by RT-PCR. Total RNA containing genomic DNA was extracted from cells as described previously (Volpe et al., 2002). Total RNA sample (~ 5 mg) was treated with 10 units of DNase I (Promega) at 37°C for 40 min, and then purified by phenol/chloroform extraction. The resultant RNA sample was subjected to RT-PCR (Onestep RT-PCR kit, Qiagen). Transcript levels in cells treated by CBZ were normalized according to those without the treatment. Data are represented as mean ± s.d.. Scale bars indicate 1 μm. (D) ChIP results showing enrichment of Cut14-Pk at the c417 locus and the centromere (cen1) in *wt* and *cut3-477* condensin mutant cells. ChIP was performed as previously described (Iwasaki et al., 2010; Noma et al., 2001), with slight modification. Chromatin was fixed with 3% paraformaldehyde followed by further cross-linking with 10 mM dimethyl adipimidate (DMA). Chromatin was sheared by Bioruptor (Diagenode). Tagged proteins were purified by mouse monoclonal anti-Pk (Serotec). Data are represented as mean ± s.d.